



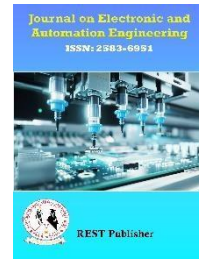
Journal on Electronic and Automation Engineering

Vol: 2(2), June 2023

REST Publisher; ISSN: 2583-6951 (Online)

Website: <https://restpublisher.com/journals/jae/>

DOI: <https://doi.org/10.46632/jae/2/2/19>



Highly Effective NB-LDPC Decoder Design on Space Telecommand Systems

***S. Ponlatha, C. Arunprasath, B. Prabakaran, S. Venkatesh Babu,**
Mahendra Engineering College, Namakkal, Tamil Nadu, India.

*Corresponding author: ponlathas@mahendra.info

Abstract: The Consultative Committee for Space Data Systems (CCSDS) currently proposes bilateral Low-Density Parity-Check (LDPC) signals and Bose-Chaudhuri-Hocquenghem (BCH) codes for correction of errors in orbit Telecommand (TC). Other possibilities, like Non-Binary LDPC (NB-LDPC) codes, were subsequently abandoned because of their high decoding difficulty. NBLDPC coding are excellent choices for interplanetary communications since they outperform their decimal equivalents over jamming and Additive White Gaussian Noise (AWGN) channels. By suggesting a very effective decoding building design, this research work demonstrate the viability of NB-LDPC coding for space TC purposes. The architecture is tailored for a space-certified Virtex-5QV FPGA, and the suggested decoding has been implemented using a (128, 64) NB-LDPC code through GF (16). At an encoded increase of 0.7 dB and a manageable installation cost, the results indicate that NB-LDPC coding is a superior substitute for the conventional binary LDPC. The suggested architecture uses just 9615 LUTs and 5637 FFs to provide a speed of 2.03 Mbps, despite the CCSDS's specified highest rate for TC being 2 Mbps (no specialized memory is employed). Furthermore, regardless of the H matrix, this architecture can be used with any standard (2, 4) NBLDPC (128, 64) code over GF (16), providing versatility in code selection. According to this work, NB-LDPC codes are a great choice for forthcoming TC uplink specification iterations.

Keywords: space communications, VLSI design, NB-LDPC codes, decoder architecture, FPGA.

1. INTRODUCTION

Shorter block-length erroneous repairing encryptions are being extensively explored and established in recent years for the transfer of TC communications in the upstream frequency of interplanetary telecommunications. The CCSDS guideline for TC synchronized and channelization [1] presently recommends a decades-old BCH as 63, 56 code and digital LDPC codes with unit sizes of (128, 64) and (512,256). The codes have more room for error to the theoretical limitations than their lengthy equivalents. As a result, higher-level decoders/code structures are often explored to close this gap in technology. CCSDS explored LDPC with Most Reliable Basis (MRB) decoding [2] as well as NB-LDPC codes. Nevertheless, those declined due to complexity of the hardware limits, which significantly limited the choice of coding channels. NB-LDPC communications have stronger encoding gain, greater explosive correction for error capability, and fewer errors floors than codes that are binary. The foregoing makes them top choices for space telecommunications. DLR [3] and NASA [4] recently suggested high-performance NB-LDPC codes. Nevertheless, these coding methods are rarely employed in practice due to the substantial equipment needs of cutting-edge systems. This study demonstrates the viability of using NB-LDPC coding for spatial TC connections as a replacement to traditional conventional LDPC codes. We present an optimized hardware implementation as 128, 64 in bits NB-LDPC decoder on GF as 16. The developed architecture is compatible with any conventional (2, 4) Parity-Check (PC) matrix of a GF as 16 NB-LDPC code with blocks width (128,64), allowing code inventers greater flexibility. The architecture is specifically tailored for a space-grade Virtex-5QV FPGA chip. The findings demonstration that the solution delivers a 0.7 dB encoding improvement ended the standard's sequential LDPC cypher while remaining relatively simple to construct. The proposed algorithm will receive discussed in the following sectors. While MRB-decoded two LDPC techniques produce a larger coding gain, their execution cost is too expensive for the needed capacity and destination expedient, as shown in the outcomes. To the finest of the researchers' expertise, currently do not exist similar

versions of small block-length NB-LDPC algorithms for space-related tasks that are reasonably priced. Increase in pressure, each leading to a specific type of martensite formation: twinned or multi-variant martensite in the former case, and twinned or single-variant martensite in the latter.

2. PROPOSED DECODING ALGORITHM

NB-LDPC recurrent algorithms rely on sending messages among constant and checking nodes across the outer boundaries of a Tanner graph. Reductions of the initial Belief Propagation (BP), also recognized as the Qary Sum-Product Algorithm (QSPA) [5], are required to lower the exorbitant amount of checking node activities. The least-grater procedure algorithm [6] is the preferred decoder technique for execution, as it works in the exponential realm. When compared to other solutions, such as BP with Fast Fourier Transform (BPFFT) [7] [8], which has the lowest decoder difficulty with an actual tiny reduction in speed. Trellis implementations of the techniques [9-11] provide greater amounts of analogy, with speeds significantly beyond those employed in telecomm and networks. Interstellar TC rates range from several hundred kbps to 2 Mbps, the maximum suggested by the CCSDS [12]. Following that, the least-grater procedure gets looked at. Suppose H represent the M x N PC matrix that defines the source code, with entries $X_{m, n}$ from Hr(s). Accept an is a representation for Gf(r). A quarry code word sent ended a binary-input AWGN network is represented by $a = (a_1; a_2; a_N)$. H(n) is a collection of checking trees related to the constant protuberance n, while M(m) is the subset of constant trees associated with the verification node m. $H_n(a)$ and $N_{post;n}(a)$ express the value of the node n's previous and subsequent knowledge about the sign. The setup set $N(m | a = a)$ can be described as the set of chains of Hr(s) signals that verify the following statement of the checking node m: $\sum_{n' \in N(m)\{n\}} h_{m,n'a_{n'}} = 0$. Signals transferred during Min-Max decryption indicate log probability ratios. The messages that are transmitted from the squared node m to the parameter node n, $Q_{m,n}$, and the communications from the mutable node n to the verify node m, $S_{m;n}$, about each sign of Hr(s) are determined and transferred in respectively repetition, till the process merges to a supreme of variations have been achieved.

Algorithm:

Initialization

A priori evidence (initial LLRs):

$$L_n(a) = \ln(P(c_n = a | channel))$$

Where S_n is the maximum probable sign for c_n

Repetitions

Squared node dispensation:

$$R_{m,n}(a) = \sum_{n' \in N(m)\{n\}} Q_{m,n'}(a_{n'})$$

Variable node processing:

$$Q'_{m,n}(a) = L_n(a) + \sum_{m' \in M(n)\{m\}} R_{m'n}(a)$$

$$Q_{m,n}(a) = Q'_{m,n}(a) - \min_{a \in GF(q)} Q'_{m,n}(a)$$

A posteriori evidence and tough choice:

$$L_{Post,n}(a) = L_n(a) + \sum_{m' \in M(n)} R_{m,n}(a)$$

The decision on C_n is $\tilde{c}_n = \arg \max_a L_{Post,n}(a)$

Proposed Architecture

The subsequent sections cover the layout of the modules that are most significant as well as the highest-level architecture. According to [13], messages have quantization with 5 bits in the recurrent method, resulting in minor speed reduction when compared to floats.

Check Node Unit (CNU)

Verify cluster computation is the most significant impediment in NB-LDPC decoder. The FB technique is composed of up of simple stages (1) that accept two source trajectories, L1 and L2, and generate a result trajectory, Lo.

$$L_o(c) = \min_{c=c_1+c_2} \max(L_1(c_1), L_2(c_2)) \quad (1)$$

To provide a successful design for calculating the fundamental min-max step, communication vectors' LLRs have been saved corresponding to their matching GF sign in power encoding [14]. It can be done to establish a fixed a connection system between least and grater contrasts by storage the LLRs of L1, L2, and Lo in shifting records confidential the least and grater component in order to take the benefit of the strength of representation (whereas a complicated changing system would be desirable required with LLRs directed in multinomial problems illustration). Furthermore, additions and dividing by H's non-zero components can be included in squared node dispensation with no expense additional than a change of the LLRs cutting-edge single of the trajectories being processed in the primary fundamental stage of the ahead and reverse stages. If this kind of method is not used, field-limited converters or cylinder shifters are necessary.

In a normal Hr. (16) NB-LDPC coding through $dc = 4$, the FB method for evaluating single check node needs calculate the elementary step six times. Figure 1 shows the data interdependence. The digits above the columns indicate that dependence column vectors designated with '1' must be estimated preceding those identified with '2'. Vectors F3 and B2 represent the initial and last outputting correspondence, correspondingly. Each message array has $q = 16$ entries (5 bits every).

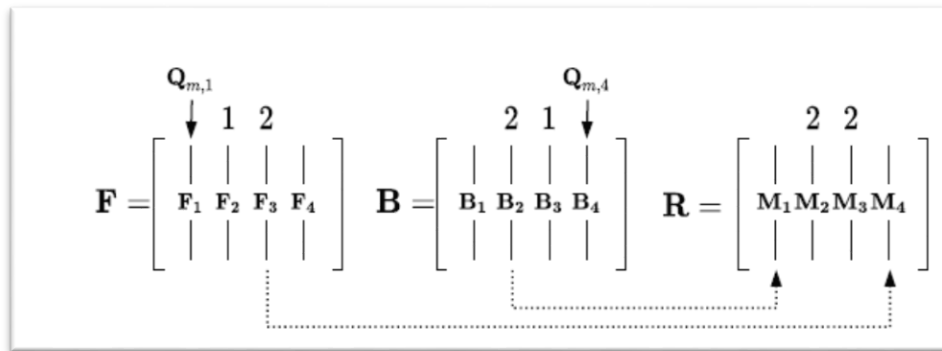


FIGURE 1. Column arrays are calculated using the forward-backward approach for the source cypher of attention ($dc = 4$) and their data dependencies.

To broaden the possibilities for for space missions at the highest encoder building construction, higher volumes and lower area implementations of the CNU and VNU are developed. The highest performance checking node design is developed with four min-max basic units, taking advantage of the maximum amount of concurrency possible. In contrast, a low-area design has only one least-grater fundamental unit in Figure. 2. We concentrate on the small area variant because we will eventually opt to employ it in the suggested decoder based on a latency-area examination. In FB sequential calculation, the advancing and reverse processes are normally analysed primary, and the consequences will be joint during the process of combining them. For the $dc = 4$ situation, we suggest a new sequencing that avoids storing the intermediate stage vectors generated in the initial backward and forward stages (F2 and B3).

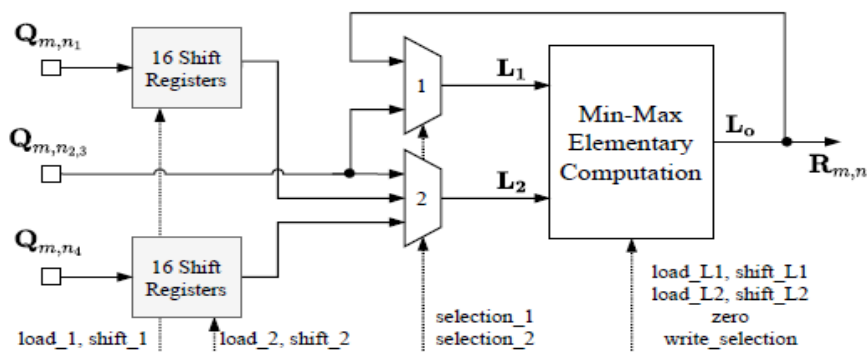


FIGURE 2. Suggested Check Node Unit CNU. Signaling provide $q=16$ -element matrices

Figure 3 depicts the updated organizing, which includes the min-max unit's input (L1; L2) and outlet (Lo) matrices at each step. In certain phases, the vectors that are supplied to L1 and L2 were changed swapped so that if a single trajectory is used in successive steps, it is required in an identical record array where it is previously kept within

the least-greater unit. Then, receiving the communications involves fewer memories being accessed. Additionally, the size of the multiplexers decreases since fewer separate communication vectors must be coupled to a single input of the min-max unit. Observe that each signal in Figure 2's topology corresponds to a $q = 16$ component vector.

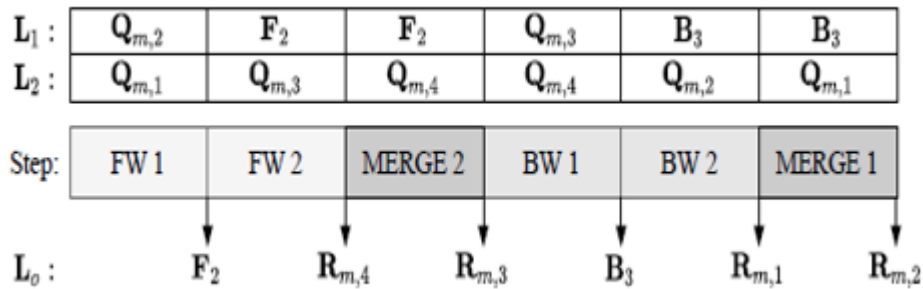


FIGURE 3. Proposed serial programming for checker node architectural with one least-greater fundamental unit.

Variable Node Unit (VNU)

VNUs with level $dv = 2$ are linked to deuce checking protuberances. The notification, Q , to be delivered to an inspection bulge is calculated by adding the notification obtained from the additional checked node to the previous channel evidence. The information vector is then adjusted, with all values being log-likelihood ratios to the single greatest probable representation. Because the smallest LLR charge is connected with the greatest likelihood, the vector's lowest value must be identified and reduced from all members. Only the previously identified signal vectors L_n will be transmitted when decryption begins. The structure shown in Figure 4 has the potential of performing the aforementioned tasks in a single minute per message. The same design is also utilized to obtain the difficult choice symbol related to the variable node with only one extra clock cycle, allowing both the logic and data generated to be reused. By saving the final sum vector in an index array, only one additional combination is required to obtain the a posteriori knowledge, and which is the most likely sign is determined by re-claiming the comparators from the tree. If the component chain has been replicated, a VNU with the smallest latency (all processes in a cycle) can be created.

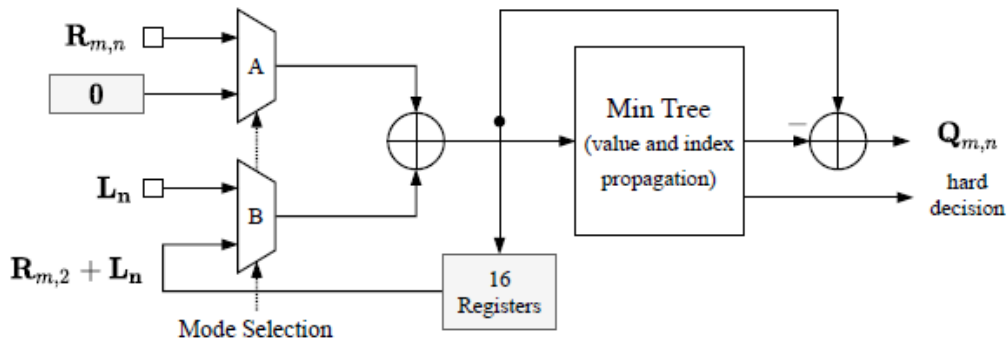


FIGURE 4. A suggested low-area architecture for a VNU. Signaling represent $q=16$ -element vectors.

Parity Check (PC) Module

During the encoding phase, it is determined if the difficult option validates all of the PC equations enforced by the validation nodes. An $rPow$ of H has four non-zero components, as $dc = 4$. Solving the m -the PC equation $\sum_{n=1}^{32} h_{m,n}c_n = 0$ gives four results and three modifications over $GF(16)$. Whenever the VNU generates an extremely difficult symbol from the provisional codeword, it is kept till all 32 characters are ready. A ROM stores all greater than zero H components as well as their positions through the matrix. Additions are performed via lookup tables, with four asynchronous ROMs encoded as reason in the FPGA LUTs. Polynomial accompaniments are performed using a bitwise XOR techniques.

General Design of the NB-LDPC Decoder

The top-level encoder design is then examined, followed by a comparison of solutions with varied latency-area ratios. The CNU and VNU components have been created with a minimum of space and delay. Additionally, various levels of parallelism can be applied. In a (128, 64) NB-LDPC coding over GF(16), the H grid measures 16 x 32. Entirely parallelism (16 CNUs and 32 VNUs) and entirely sequential systems can be created with either minimum space or delay elements. They are depicted in the latency-area graph in Figure 5. Except for specific circumstances, these extreme solutions will be avoided in practical implementations. In the meantime, various partial-parallel designs with a more beneficial compromise emerge. Designs with 8 with 16 CNUs and 1-to-8 VNUs are especially effective because they are positioned closer to the graph's source. Partial-parallel designs, as shown in Figure 5, are designed using small area components because they satisfy normal TC throughputs while requiring the fewest resources from the hardware. The graph does not include the area cost from recollections, connectivity, or control. The required extra funds have little effect on and impact every choice in the same manner

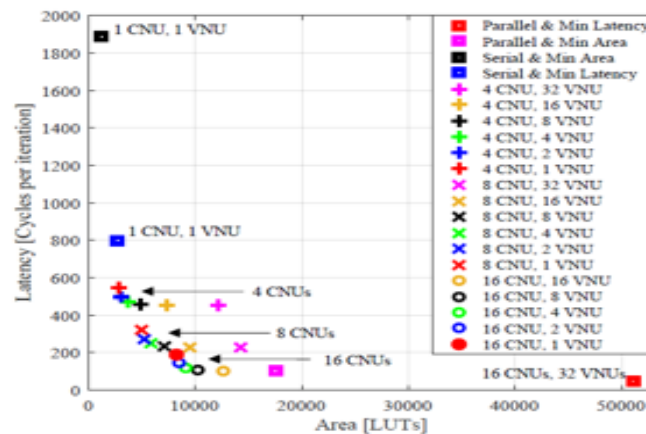


FIGURE 5. Area-latency analysis of possible designs for implementing the (128, 64) NB-LDPC decoding on GF(16).

The enterprise with 16 CNUs and 1 VNU, represented by an enflamed solid rectangle in Figure 6, is selected for execution. It is the smallest-area option that meets the 2 Mbps limit. For determining the rate of data transfer, a maximum of 18 decoder cycles were used, with effectiveness provided in Section IV. Designs with less CNUs do not meet the speed requirements, and employing less decode repetitions rapidly results in efficiency loss. The selected point offers certain further benefits over various other designs. First, designs with 16 CNUs do not require massive switch registers at the CNUs' inputs since the shift can be programmed according to the separate CNU for each single column of H. Secondly, employing only one specialized VNU reduces connectivity cost between units and communication memory, allowing certain expensive multiplexors to be eliminated. The previous knowledge is stored in one RAM, while the algorithmic instructions are stored in 16 dual port RAMs, allowing each CNU to read and write information in simultaneously. Furthermore, the (16 CNUs, 1 VNU) design has the benefit of being compatible with slightly (128, 64) NB-LDPC software with $(dv; dc) = (2; 4)$ across GF(16) with without memory problems or architectural modifications. As a consequence, functionality designers might suggest focused on results tweaks or unique code while remaining within the exact same design. Other partial-parallel designs may offer challenges, such as multiple VNUs requiring access to a single message in memory (where rows being processed simultaneously contain non-zero values from the similar row of H). This could end up in more equipment, delays, and a modification of the management logic. Figure 6 shows a diagram of the suggested top-level design.

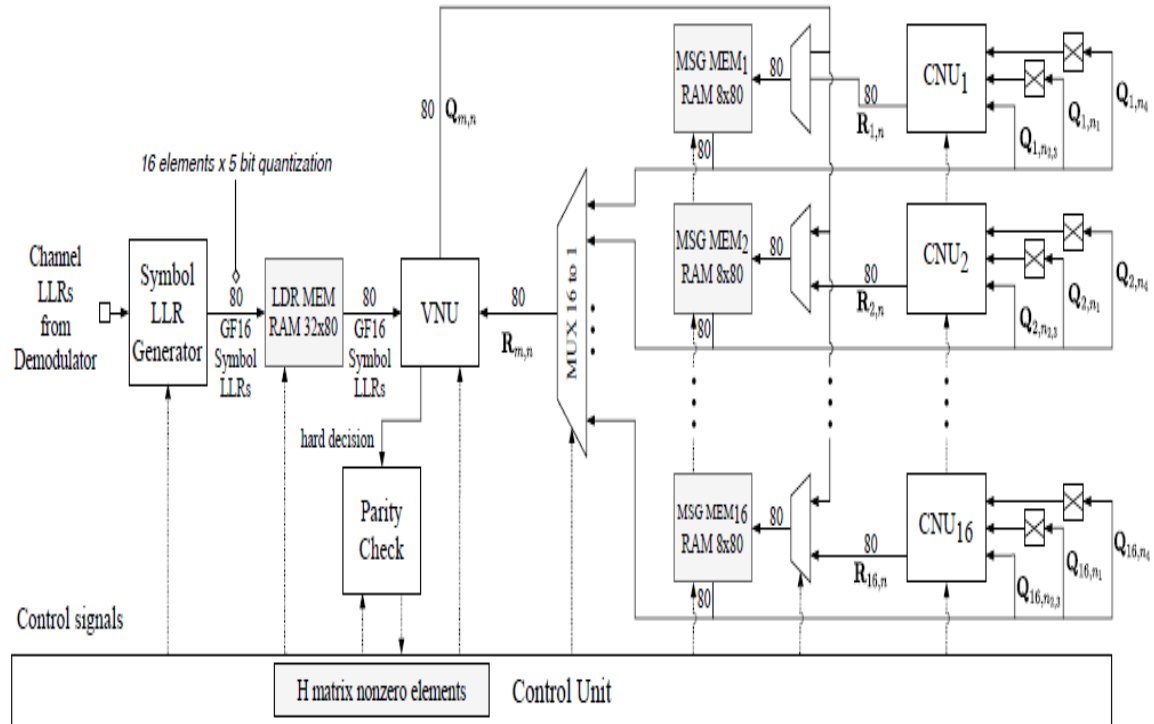


FIGURE 6. An overview of the planned NB-LDPC decoding design. Signals provide $q = 16$ component vectors

Implementation Results

Figure 7 depicts the Codeword error rate (CER) of an NB-LDPC coding ended GF (16) with values 128, 64 bits across a double contribution AWGN network. The PC matrix for the NBLDPC code was produced using a variation of the continuous edge development procedure. Figure 7 shows the outcome of (i) the QSPA and least-greater floating-point computing designs, (ii) the suggested quantified least-greater execution, and (iii) the CCSDS double LDPC coding with quantization deciphering - with an optimal number of 200, 18, and 90 decryption repetitions, correspondingly. In quantized versions, the iteration limitation is set to match the desired capacity for the highest total repetitions while compromising only a small amount of speed. Interestingly, the NB code has an enciphering increase of 0.7 dB above its conventional rival from the CCSDS specification. Our version employs 9615 Slice LUTs as 12.6% and 5726 FFs as 7.8% as 6.9% on a space-grade Virtex-5QV FPGA. The obtained bandwidth is 2.03 Mbps, which surpasses the current indicated maximum of 2 Mbps for CCSDS providers in high-speed TC communications. Using specialized BRAMs would necessitate data replication as a space safety mechanism. Rather, memories are utilized as distributed storage in radiation-protected FPGA logic. As a result, reminiscences are incorporated in the aforementioned LUT usage. The additional support summarizes the execution of the double LDPC code as it now exists in the normal. The architecture consumes been area improved with standardized min-sum decode and the same 2 Mbps limitation. In the third base section, we discuss double LDPC with MRB deciphering, which is driven by its excellent error correction features. The authors in [2] describe the number of computing components to be employed, supposing a maximum speed constraint of 1 Mbps and a rate of execution of 100 MHz. The number needed LUTs and FFs exceeds the number readily accessible on an intended FPGA, indicating that the MRB approach is only practical for considerably slower purposes.

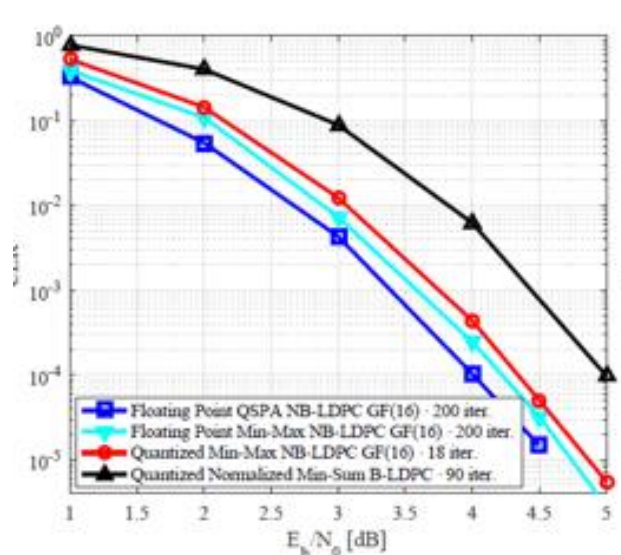


FIGURE 7. Effectiveness of the suggested least-greater implementation for the (128, 64) NB-LDPC code done GF (16), using a frequency with AWGN and BPSK encoding.

3. CONCLUSION

This paper introduces a successful design that demonstrates the possibility of NB-LDPC encoding for improvement of errors in interplanetary TC transmissions. This technique exceeds the conventional LDPC code on both AWGN and jamming communications. Regardless of the fact that NB-LDPC codes weren't comprised in the CCSDS suggestion for TC because of their substantial deciphering difficulty, the suggested decoder surpasses the CCSDS recommended maximum speeds of 2 Mbps for TC hyperlinks whereas using solely 9615 LUTs and 5637 FFs on a Virtex-5QV FPGA. To the greatest extent of our understanding, this is the very primary application of short block-length NB-LDPC codes for interplanetary TC networks at an affordable price. The findings of this study suggest that NB-LDPC cyphers are a viable choice for the next edition of the CCSDS normal.

REFERENCES

- [1]. CCSDS 231.0-B-3. "TC Synchronization and Channel Coding". Blue Book, Sep. 2017.
- [2]. M. Baldi et al., "On the use of ordered statistics decoders for low-density parity-check codes in space telecommand links", *Journal Wireless Communications and Networking* 2016, Art. 272, Nov. 2016.
- [3]. G. Liva et al., "Codes on high-order fields for the CCSDS next generation uplink", *Advanced Sat. Mult. Systems Conf. (ASMS) and Signal Proc. Space Comm. Workshop (SPSC)*, Baiona, 2012, pp. 44-48.
- [4]. B. Chang, D. Divsalar and L. Dolecek, "Non-binary protograph-based LDPC codes for short block-lengths", *2012 IEEE Information Theory Workshop, Lausanne, Switzerland, 2012*, pp. 282-286.
- [5]. M. C. Davey and D. MacKay, "Low-density parity check codes over GF (q)", *IEEE Commun. Letters*, vol. 2, no. 6, pp. 165-167, Jun. 1998.
- [6]. V. Savin, "Min-Max decoding for non-binary LDPC codes", *Proc. IEEE Intl. Symp. On Info. Theory, Toronto, Canada, Jul. 2008*.
- [7]. L. Barnault and D. Declercq, "Fast decoding algorithm for LDPC over GF (2q)", *Proc. IEEE Inf. Theory Workshop, Paris, 2003*, pp. 70-73.
- [8]. D. Declercq and M. Fossorier, "Decoding Algorithms for Nonbinary LDPC Codes Over GF(q)", *IEEE Transactions on Communications*, vol. 55, no. 4, pp. 633-643, Apr. 2007.
- [9]. E. Li, K. Gunnam and D. Declercq, "Trellis based Extended Min-Sum for decoding nonbinary LDPC codes", *ISWCS, Aachen, 2011*, pp. 46-50.
- [10]. Y. Ueng et al., "A High-Throughput Trellis-Based Layered Decoding Architecture for Non-Binary LDPC Codes Using Max-Log-QSPA" *IEEE Transactions on Signal Processing*, vol. 61, no. 11, pp. 2940-2951, 2013.
- [11]. M. Li et al., "An Efficient High-Rate Non-Binary LDPC Decoder Architecture with Early Termination", *IEEE Access*, vol. 7, 2019.
- [12]. CCSDS 401.0-B-28. "Radio Frequency and Modulation Systems – Part 1". Blue Book, Feb. 2018.
- [13]. X. Zhang and F. Cai, "Efficient Partial-Parallel Decoder Architecture for Quasi-Cyclic Nonbinary LDPC Codes", *IEEE Transactions on Circuits and Systems I: Regular Papers*, vol. 58, no. 2, pp. 402-414, Feb. 2011.
- [14]. F. Cai and X. Zhang, "Efficient Check Node Processing Architectures for Non-binary LDPC Decoding Using Power Representation", *2012 IEEE Workshop on Signal Processing Systems*, pp. 137-142, Oct. 2012.